Electric field induced reversible spreading of droplets into films on lubricant impregnated surfaces

This manuscript was accepted by Appl. Phys. Lett. Click here to see the version of record.

Zuzana Brabcova,[a] Glen McHale[a] and Gary G.Wells

Smart Materials and Surfaces Laboratory, Faculty of Engineering & Environment, Northumbria University, Ellison Place, Newcastle upon Tyne, NE1 8ST, United Kingdom

Carl V. Brown, Michael I. Newton

School of Science and Technology, Nottingham Trent University, Clifton Lane, Nottingham, NG11 8NS, United Kingdom

a) corresponding authors: z.brabcova@northumbria.ac.uk, glen.mchale@northumbria.ac.uk

Abstract

Electric fields can be used to force a droplet to wet a solid surface using an applied voltage. However, significant hysteresis usually occurs associated with pinning forces at the contact line. Here we report the forced spreading and subsequent retraction of droplets into liquid films in air on lubricant impregnated surfaces (also known as slippery liquid infused porous surfaces, SLIPS) where the contact line is completely mobile. We first confirm that we achieve a complete removal of hysteresis for the electrowetting of droplets above the saturation voltage. We then show that contact angle hysteresis can be reduced to less than 4° whilst retaining the ability to fully spread a droplet into a liquid film using an interface localized from of liquid dielectrophoresis (dielectrowetting). In both cases, we find that the cosine of the contact angle has a quadratic dependence on applied voltage, consistent with previous theoretical expectations. Thus, our work demonstrates that fully reversible spreading encompassing a wide range of partial wetting droplet states and a film state can be achieved in air in a controllable manner with very low levels of hysteresis.

Keywords

Electrowetting, dielectrowetting, droplets, contact angles, lubricant impregnated surface, SLIPS.

Electric fields have proved important in manipulating[1] and controlling droplets[2] of

conducting and dielectric liquids with applications in liquid lenses,[3] optofluidics[4] and droplet microfluidics[1,2,5,6]. Two of the reported approaches are electrowetting, which manipulates the ions in a conducting liquid droplet at the solid-liquid interface and stores capacitive energy by the polarization of a solid dielectric layer[7–9]. Another one is dielectrowetting, which manipulates dipoles in a dielectric liquid droplet at the solid-liquid interface to store capacitive energy by polarizing a liquid dielectric layer.[10–12] There are significant limitations in the electrowetting approach including the need for any liquids of interest to be conducting and typically the need for direct electrical contact with the liquid, although there are examples of using non-contacting co-planar electrodes.[13,14] However, the major limitation is an inability to spread a droplet to a film state, due to the existence of a minimum saturation contact angle, θ_{sat}.[9,15]

Dielectrowetting utilizes the dielectric properties of liquids, but the effect is localized to the interface[16], and can be used to induce spreading or superspreading of droplets of non-conducting liquids.[11,16] Moreover, the saturation of contact angle appears lower than in the case of electrowetting[11] and it is possible to achieve the full range of wetting from a droplet to a film state that has not been reported in the case of electrowetting.[9,17,18] Full wetting has been shown to be useful for optical applications based on controlled changes to the shapes of films of liquids.[16,19,20] However, in both the electrowetting and dielectrowetting approaches in air the solid surface causes a hysteresis in which the contact angle does not recover its original value over the course of several cycles of increasing and decreasing voltage. In electrowetting, one approach to removing hysteresis is to operate with a droplet immersed in a second immiscible liquid, such as an oil,[21ref] and this can result in an entrapped film between the substrate and the droplet.[22ref] Such droplet-in-liquid systems can allow

properties, such as interfacial tension and density contrast (e.g. for neutral buoyancy[7]), to be

tailored for practical applications.

In recent work, it was reported that contact angle hysteresis could be removed when electrowetting in air on lubricant impregnated surfaces[23] (also referred to as a slippery liquid infused surface - SLIPS[24,25]). The focus in that work was on achieving a completely reversible and tuneable liquid lens with improved transient response due to reduced droplet oscillations. Limited information on the agreement with theory between contact angle and applied voltage was provided, and the persistence of a saturation contact angle precluded film formation. In our work, we confirm that electrowetting on a SLIP surface in air obeys the modified Young's law for electrowetting but with no hysteresis. Moreover, we show that dielectrowetting with very low levels of hysteresis can be achieved, when spreading between a droplet and film state, in a completely reversible manner. We show good correlation with theoretical expectations and without breakdown of the lubricant impregnated surface.

To investigate electrowetting, we used the system shown in **FIG. 1a**. A gold conductive layer (100 nm) was deposited on a glass substrate and coated with an insulating capping layer of photoresist SU8-2002 (MicroChem, 1.22, 1.57 and 2.05 µm, ε_r=3) which can withstand ~550 V before electrical breakdown. For dielectrowetting studies, a four arm spiral electrode device with electrodes of width d, separated equidistantly by gaps of d, activated by a four phase signal approach was used (**FIG. 1b**).[10] Because the penetration depth of the electric field into the liquid is related to the electrode-gap sizes, samples with electrode sizes of d=60, 80, 100, 120 and 180 µm were made. The capping layer used (1.22 µm) was identical to the one for electrowetting to ensure uniformity and comparable wetting properties. This capping layer protects against electrolysis of the liquid and subsequent destruction of a device should the droplet becomes conductive for any reason (e.g. when using hygroscopic liquids).
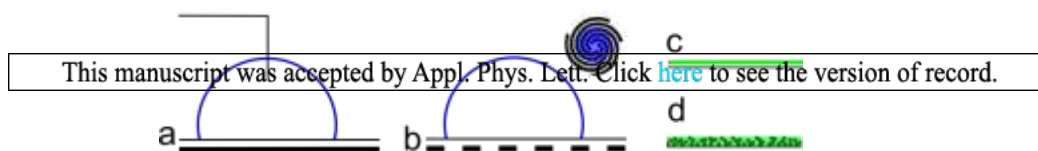
FIG. 1. (a) Schematic of a droplet in an electrowetting setup (b) Schematic of a dielectrowetting system. Inset: Top view of a spiral electrode pattern, (c) Sketch of a hydrophobic layer; (d) Sketch of a Slippery Liquid Infused Porous Surface.

Two types of surfaces were investigated. In the first case, a hydrophobic layer of Novec 1700[TM] (3M[TM], 0.3 μm, ε_r=3, fluoropolymer oleophobic coating) was applied to the surface to achieve a high initial contact angle (>90°) for both water and glycerol and thus provide a hydrophobic surface (**FIG. 1c**). In the second case, a slippery lubricant impregnated surface was created by applying a commercial solution containing nanoparticles (Glaco Mirror Coat) to create a superhydrophobic surface and then infusing it with silicone oil (Sigma-Aldrich, 20 cSt). The silicone oil was applied by dip coating at 1mm s^{-1} thereby resulting in an oil infused layer of thickness 15 μm (**FIG. 1d**). Droplets of glycerol on this surface were observed to slide when the surface was tilted from the horizontal by ca.0.8°.

Electrowetting experiments were performed using a sinusoidal AC voltage and the electrical addressing in the dielectrowetting experiements was performed using the four phase AC actuation previously described in Brabcova *et al*[10]. All sets of experiments were performed with droplets in air. For dielectrowetting experiments, droplets of glycerol were carefully dispensed onto the electrodes (typical volume of 5 μl), and both side and top view images were recorded. Since pure glycerol is a hygroscopic liquid (99.5%, Sigma Aldrich) it was stored in a perfectly sealed container and a fresh droplet was used for every experiment. The operating frequency was 10 Hz for electrowetting and 1000 Hz for dielectrowetting. Since the capillary length for glycerol is $\kappa^{-1}=(\gamma_{LV}/\rho g)^{1/2}$=2.3 mm, where γ_{LV} is the surface tension, ρ, the density and g the acceleration due to gravity, droplets have an initial (zero applied

voltage) profile which is slightly gravitationally flattened. We verified that the liquid was

exhibiting a dielectric response consistent with expectations of operating above a relaxation frequency of ionic motions of 14 Hz. This is needed for dielectrophoresis to dominate based on a permittivity of 42.5 and conductivity of 5.6×10^{-8} S m^{-1}.[8] For electrowetting experiments, the number of free ions in glycerol was increased by the addition of NaCl (0.13 mol l^{-1}) giving a conductivity of 1.7×10^{-6} S m^{-1}. This is to ensure ionic migration, which creates the polarisation of charge across the dielectric surface, did occur for the applied voltage and frequency used.

Top view images (dielectrowetting experiments) were captured with a Canon D600 fitted with a macro objective (Carl-Zeiss Jena, Pancolar). Side profile view images were captured using a Krüss Drop Shape Analysis system (DSA30) with the apparent contact angles measured by fitting an ellipse to the droplet profile. Thus, all contact angles discussed in this work are macroscopic ones rather than microscopic ones, which may differ at length scales significantly smaller than the electric field penetration depth, set by the electrode size. The advancing contact angle of glycerol droplets on the hydrophobic and SLIP surface measured by the volume addition method was 104.0°±0.9° and 95.0°±0.8°, respectively, and the corresponding receding angles were 89.0°±1.2° and 94.0°±0.9° for these surfaces.
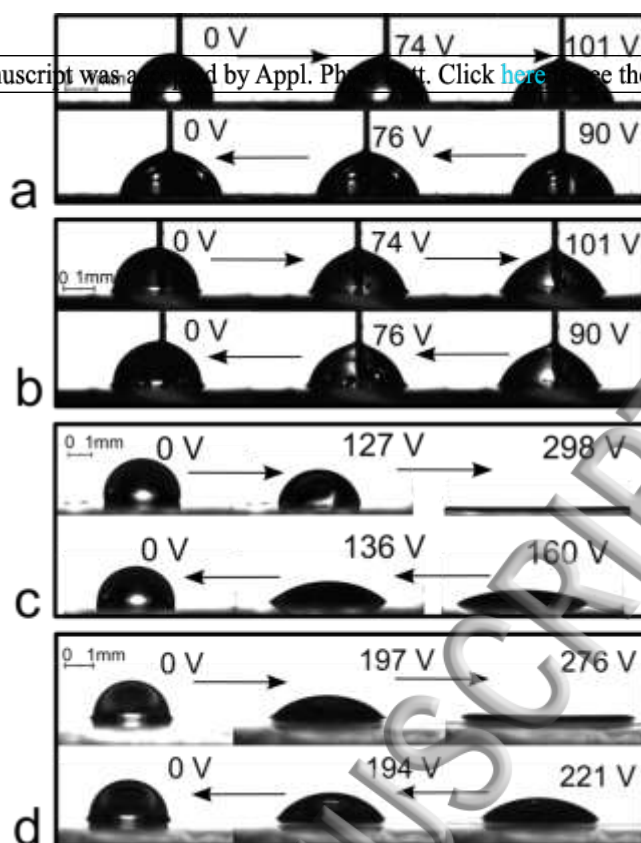
FIG. 2. (a,b) Side view images of droplet of glycerol under electrowetting – (a) hydrophobic surface, (b) SLIP surface. (c,d) Side view images of a droplet of glycerol on a spiral dielectrowetting device with $d=100$ μm showing the effect of (c) hydrophobic layer, (d) SLIPS. All voltages are provided as rms values.

Figure 2 shows electrowetting (**a**,b) and dielectrowetting (**c,d**) on hydrophobic (**a,c**) and SLIP surfaces (**b,d**). Electrowetting experiments on both hydrophobic and SLIP surfaces exhibited contact angle saturation with the contact angle decreasing from 98°±0.7° for the hydrophobic and 90.0º±0.5º for the SLIP surface to a minimum of ~70-75° (**FIG. 2a,b**). However, in contrast to the hydrophobic surface, on the SLIP surface the droplet fully retracts back to its original state as the voltage is removed (**FIG. 2b**). For dielectrowetting the droplet spreads into a film state on both types of surfaces (**FIG. 2c,d**) and on the SLIPS surface, it is able to fully recover its shape through a sequence of smooth changes as the applied voltage is reduced (**FIG. 2d**).
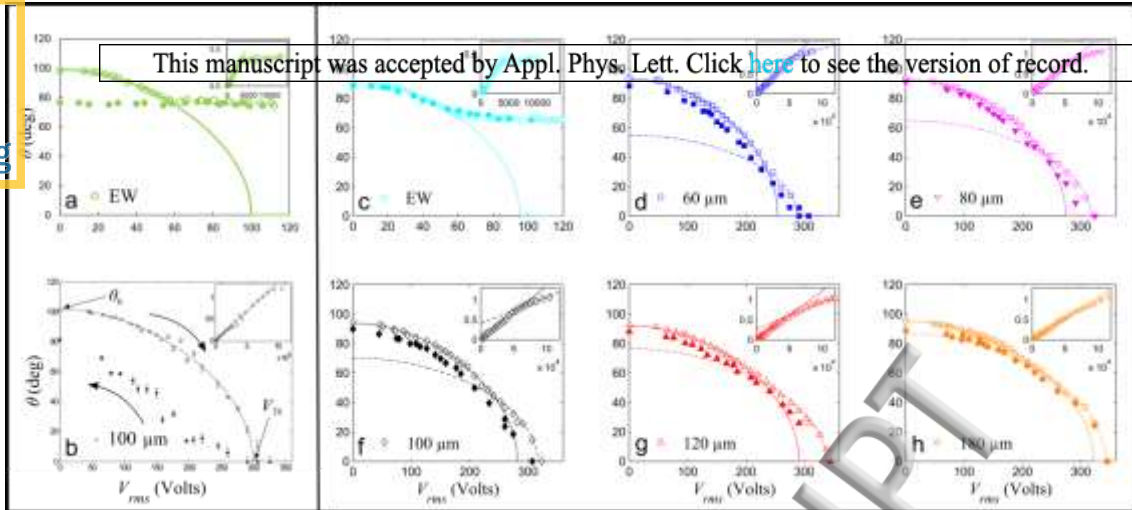
FIG. 3. The contact angle-voltage relationship for the increasing (open symbols) and decreasing (filled symbols) voltage half-cycles for (a,c) electrowetting and (b,d-h) dielectrowetting for all electrode sizes (d=60, 80, 100, 120, 180 μm). Inset: data plotted as $\Delta\cos\theta=\cos\theta(V_{rms})-\cos\theta(0)$ versus (rms) voltage squared; the solid lines are fits using data with contact angles above 20°. (a,b) hydrophobic surface, (c-h) Slippery Liquid Infused Porous Surface.

Figure 3 shows both an increasing voltage half-cycle and a decreasing voltage half-cycle for electrowetting and dielectrowetting (using d=100 μm as an example) using the hydrophobic and SLIP surfaces. In each case, the inset plots show $\Delta\cos\theta=\cos\theta(V_{rms})-\cos\theta_0$ as a function of the square of the rms voltage, V_{rms}^2, and therefore tests its linearity. In each of the dielectrowetting on SLIPS cases (**Fig. 3d-h**), linear fits have been taken over data points in the higher and lower voltage ranges and these two fits then combined to show the solid curves in the main figure in each panel. The critical voltage (and the related contact angle) represents the cross-over voltage between the linear fits to lower and higher voltage ranges as shown in each inset. The shift of this point and its dependence on the electrode size may help understand the origin of such saturation effects in electrowetting.[7,18] In the case of the hydrophobic surfaces (**Fig. 3a,b**) the droplet shape changes smoothly for the increasing voltage half-cycle, but either pins and is unable to recover (electrowetting; **Fig 3a**) or involves jumps during the contact line retreat as the droplet pins and unpins (dielectrowetting; **Fig. 3b**). In both electrowetting and dielectrowetting there is a significant

7

contact angle hysteresis problem with droplets not recovering their initial contact angles

when the voltage is removed. The situation on a SLIP surfaces contrasts sharply with either complete removal of hysteresis (electrowetting; **Fig. 3c**) or a much reduced hysteresis to 3-4° (dielectrowetting; **Fig. d-h**) and smooth retraction of the contact line. Comparing **Fig. 3d-h**, we observed that as the size of the electrodes increases, the critical point is shifted towards lower voltages (and higher contact angles).
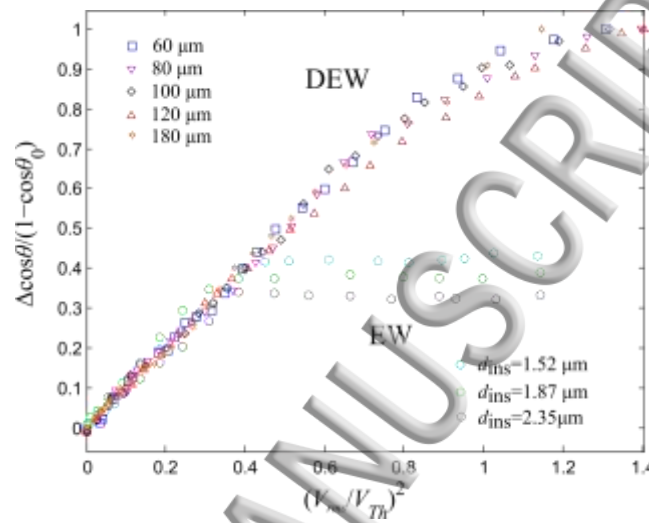

FIG. 4. Scaling comparison of data in **FIG. 3** showing the range where electrowetting and dielectrowetting respect the quadratic dependence of $\Delta\cos\theta$ on V_{rms}^2.

The full data set for electrowetting and dielectrowetting can be collapsed onto one master curve using axes scaled based on the initial contact angle, θ_o, and a projected threshold voltage, V_{Th}, corresponding to a zero degree contact angle based on the quadratic fit between $\cos\theta$ and V_{rms}^2.[4,10] **Figure 4** shows the scaling result using an x-axis of V_{rms}^2/V_{Th}^2 and a y-axis $\Delta\cos\theta/(1-\cos\theta_o)$. It is possible to estimate which of these methods respects the electrowetting or dielectrowetting modified Young's law over five different strengths of dielectrowetting defined by the electrode size, d, and three different strengths of electrowetting defined by the insulator thickness.

8

Our results show lubricant impregnated/SLIP surfaces can be used to eliminate or reduce

hysteresis without altering the basic contact angle – voltage relationship observed on simple solid surfaces. For electrowetting we observed excellent agreement with no hysteresis over the range of droplet states defined by the saturation contact angle. We then showed that dielectrowetting was able to reduce contact angle hysteresis to ~3-4° whilst retaining the ability to reversibly spread a droplet into a film and without displacing the lubricant from the surface. Since this approach can achieve reversible low hysteresis control between a droplet and a film state in air without mechanical parts and in a scalable manner, it may be significant for liquid-based optics,[4,19,20] droplet-based microfluidics,[26] and related applications[21].
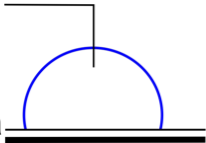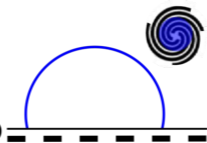
Acknowledgement

References

[1] M.G. Pollack, R.B. Fair, and A.D. Shenderov, Appl. Phys. Lett. **77**, 1725 (2000).

[2] P. Paik, V.K. Pamula, M.G. Pollack, and R.B. Fair, Lab Chip 28 (2003).

[3] B. Berge and J. Peseux, Eur. Phys. J. E **3**, 159 (2000).

[4] G. McHale, C. V Brown, M.I. Newton, G.G. Wells, and N. Sampara, Opt. Des. Test. V **8557**, 1 (2012).

[5] K. Xie, Y. Lai, X. Guo, and R.J. Campbell, Microsyst. Technol. **17**, 367 (2011).

[6] A. Torkkeli, (2003).

[7] F. Mugele and J. Baret, J. Phys. Condens. Matter **17**, (2005).

[8] T.B. Jones, Langmuir **18**, 4437 (2002).

[9] F. Mugele, Soft Matter **5**, 3377 (2009).

[10] Z. Brabcova, G. McHale, G.G. Wells, C. V. Brown, M.I. Newton, and A.M.J. Edwards, Langmuir **32**, 10844 (2016).

[11] G. McHale, C. V Brown, M.I. Newton, G.G. Wells, and N. Sampara, Phys. Rev. Lett. **107**, 1 (2011).

[12] C. V Brown, G.G. Wells, M.I. Newton, and G. Mchale, Nat. Photonics **3**, 8 (2009).

[13] U.-C. Yi and C.-J. Kim, J. Micromechanics Microengineering **16**, 2053 (2006).

[14] A.G. Banpurkar, K.P. Nichols, and F. Mugele, Langmuir **24**, 10549 (2008).

[15] J. Heikenfeld and M. Dhindsa, J. Adhes. Sci. Technol. **22**, 319 (2008).

[16] G. McHale, C. V Brown, and N. Sampara, Nat. Commun. **4**, 1 (2013).

[17] A. Quinn, R. Sedev, and J. Ralston, J. Phys. Chem. B **109**, 6268 (2005).

[18] S. Chevalliot, S. Kuiper, and J. Heikenfeld, J. Adhes. Sci. Technol. **26**, 12 (2012).

[19] R. Zhao, B. Cumby, A. Russell, and J. Heikenfeld, Appl. Phys. Lett. **103**, 1 (2013).

[20] A. Russell, E. Kreit, and J. Heikenfeld, Langmuir **30**, 5357 (2014).

[21] R.A. Hayes and B.J. Feenstra, Nature **425**, 383 (2003).

[22] A. Staicu and F. Mugele, (n.d.).

[23] C. Hao, Y. Liu, X. Chen, Y. He, Q. Li, K.Y. Li, and Z. Wang, Sci. Rep. **4**, (2014).

[24] J.D. Smith, R. Dhiman, S. Anand, E. Reza-Garduno, R.E. Cohen, G.H. McKinley, and K.K. Varanasi, Soft Matter **9**, (2013).

[25] T. Wong, S.H. Kang, S.K.Y. Tang, E.J. Smythe, B.D. Hatton, A. Grinthal, and J. Aizenberg, Nature **477**, 443 (2011).

[26] M.G. Pollack, R.B. Fair, and N. Carolina, **77**, 1725 (2000).

a b c d

a

0 V   74 V   101 V

0 V   76 V   90 V

b

0 V   74 V   101 V

0 V   76 V   90 V

c

0 V   127 V   298 V

0 V   136 V   160 V

d

0 V   197 V   276 V

0 V   194 V   221 V

0 1mm

Figure panels (a)–(h) showing θ (deg) versus V_{rms} (Volts).

- (a) EW
- (b) θ_0, V_{Th}, 100 μm
- (c) EW
- (d) 60 μm
- (e) 80 μm
- (f) 100 μm
- (g) 120 μm
- (h) 180 μm